applied sciences

MDPI

Article

Experimental Verification of Use of Vacuum Insulating Material in Electric Vehicle Headliner to Reduce Thermal Load

Soo-Whang Baek, Sang Wook Lee and Chul-Soo Kim *

Department of Automotive Engineering, Honam University, 417 Eodeung-daero, Gwangsan-gu, Gwangju 62399, Korea; swbaek@honam.ac.kr (S.-W.B.); swlee@honam.ac.kr (S.W.L.)
* Correspondence: kimcs@honam.ac.kr; Tel.: +82-62-940-5401

Received: 26 September 2019; Accepted: 3 October 2019; Published: 9 October 2019

check for updates

Abstract: In electric vehicles (EVs), the use of high-temperature heat transfer components that effectively block external heat and minimize cooling losses can increase vehicle mileage during heating/cooling operations and improve passenger comfort. In particular, in ensuring high thermal insulation, the car headliner forms an important component for effectively managing environmental heat energy and heating and cooling processes inside the EV. In this study, we have proposed and experimentally verified the use and efficacy of vacuum insulation material in the headliner of EVs to reduce the heat load. The thermal conductivity and air permeability of various conventional insulating and vacuum insulation materials used for the headliner were compared to accurately predict the vacuum insulation material performance. We found that the vacuum insulation material affords reduced surface roughness and thermal conductivity and high formability relative to conventional insulation. We also confirmed consequent improvements in the insulation performance by comparing the characteristics of the proposed vacuum-insulation-material headliner (relative to conventional materials) via prototyping and reliability testing. With the "improved" headliner, in summer, the temperature of the automobile cabin was lowered by 2.8 °C, and the cabin temperature was lowered by 3.9 °C during the cooling period relative to conventional insulators, which proves that the cabin temperature can be maintained at a low value during summer parking or cooling. In winter, the cabin temperature was found to be 7.7 °C higher than that obtained with the conventional insulator, which indicates that the cabin temperature can be maintained higher via reduction in the heat loss (because of using vacuum insulation) under the same heating energy conditions during winter.

Keywords: electric vehicle; heat insulating material; heating; cooling; interior material; headliner

1. Introduction

The main obstacle to the commercialization of electric vehicles (EVs)—environmentally friendly cars—is that they offer lower mileage for a single charge when compared with the mileage of internal combustion engines [1–4]. For vehicles with internal combustion engines, the vehicle cooling operation reduces fuel consumption by 20–30%, thereby reducing the mileage by 2%–30%; on the other hand, in the case of heating, fuel consumption is not affected as the waste heat of the engine is used [5–7]. However, in the case of an EV in which the waste heat source is relatively small, electrical power consumption caused by electrical heating decreases the mileage by about 30–50% [8–10]. Thus, small EVs are currently being designed for urban driving to achieve a target driving distance of 140–160 km per charge.

As of today, city-based small EVs are not commercially viable owing to their long charging time and lack of charging infrastructure, and thus, car manufacturers are striving to secure the EV technical capabilities in this context [11–13]. Therefore, the comprehensive development of power-saving technology for heating and cooling operations in lieu of increasing the mileage has become essential for EV development. Currently, there is a need for efficient EV development strategies to reduce heating and cooling power consumption and increase the mileage per charge [14–16].

In order to increase the distance that the vehicle can travel during the heating/cooling operation and to improve passenger comfort, heat from outside the vehicle must be blocked effectively. Therefore, there is a need for using suitable thermal insulation management components that can minimize cooling and heating energy loss within the vehicle interiors [17–19].

Here, we note that the aesthetic quality, as well as thermal loading capacity, of automotive parts in a vehicle's interiors can directly impact passenger comfort. The headliner is an internal part on the roof of the vehicle, which affords good sound absorption and sound insulation performance to prevent outside noise or engine noise from entering the passenger cabin, thus enhancing passenger comfort. Further, the headliner also acts as a safety barrier for passengers in the case of a collision. However, thus far, the headliner has not been recognized as a product that can significantly contribute to the driving performance of the vehicle. In the stage of product development, the headliner is normally considered only in terms of its appearance, design sensibility, and stability; its insulation performance is not considered [20–22]. Consequently, this study examines the thermal insulation capacity of the headliner.

The headliner is attached to the body panel of the vehicle. However, owing to its thickness and shape limitations, it is very difficult to improve its insulation performance (and that of internal components in general) with the use of common insulation materials. Further, regarding the enhancement of the heat insulating performance, the use of conventional heat insulating materials as the built-in component increases the overall volume and weight. In addition, the temperature within the vehicle cannot be easily managed, due to the heat released from the heat insulating material after a certain duration. Therefore, it is necessary to use materials with suitable thermal properties, such as vacuum insulation materials. Unlike conventional insulation, vacuum insulation creates a vacuum inside the headliner, and heat transfer is blocked because of the vacuum structure. The resulting heat insulating performance is better than that of conventional heat insulating materials, and even for low material thicknesses, the heat insulating performance is equivalent to or greater than that of existing heat insulating materials [23–26].

Against this backdrop, in this study, we used a vacuum insulator to improve the surface roughness and thermal conductivity of the headliner and the overall insulation performance. In order to improve the moldability of the vacuum insulator, we increased the degrees of freedom for forming the vacuum insulator by applying a molding method wherein the getter in the insulation is uniformly coated with the core material without being sealed. By reducing the surface roughness, the possibility of breaking the vacuum insulation when attaching the skin layer is reduced. In our thermal conductivity measurements, we found that the vacuum insulation thermal conductivity varied according to the measured temperature range. Further, the thermal conductivity at each evaluated temperature exhibited an improvement relative to conventional materials, which proves the reliability of our approach. With the vacuum-insulation headliner, we measured the temperature change in the interior of the cabin in addition to the battery consumption, and we found that the use of high-thermal-insulation internal components also improved the surface temperature of the internal parts. When our high-thermal-insulation material was applied, the surface temperature of the interior material increased and decreased during heating and cooling operations, respectively. The internal heat energy loss was reduced because of the smaller heat loss due to better heat insulation. In addition, because the headliner is positioned close to the passenger, it can be expected that the resulting enhanced cooling and heating effects can afford increased passenger comfort.

2. Vacuum Insulator for Electric Vehicle Headliner

Figure 1 shows the configuration of the interior of an EV. In general, car interiors play a role in improving passenger comfort depending on the design and function, and simultaneously they play an important role in interior noise reduction. Further, they also aid in improving fuel economy and reducing energy consumption via weight minimization. In the past, research and development on components such as the hood, dash, fender insulator, insulation (ISO)-dash pad and headliner have aided in minimizing noise inflow into the cabin and protecting the vehicle. We note that existing studies on automobile interior materials have mostly focused on their crash stability and sound insulation performance; studies on reducing the thermal load using automobile interior materials are lacking.

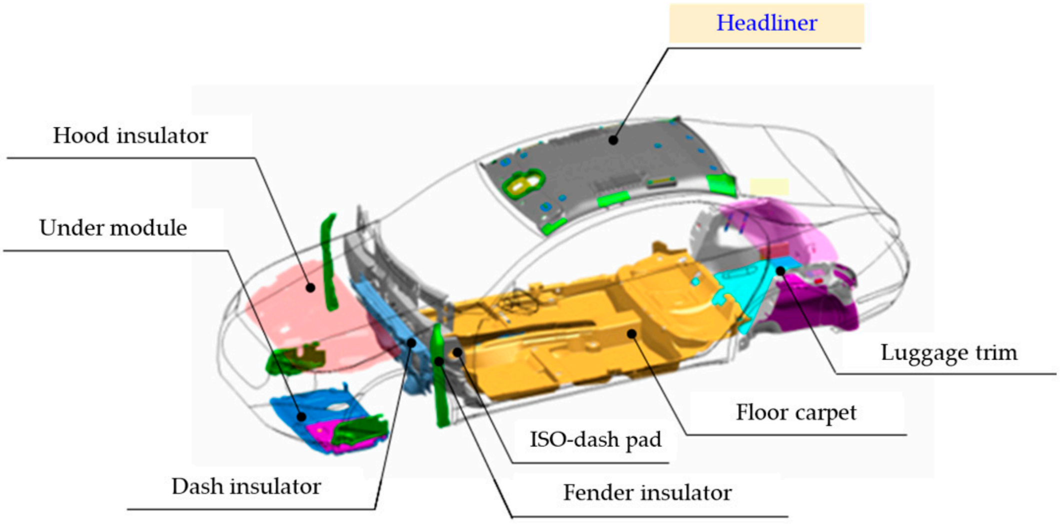

Figure 1. Material configuration of electric vehicle interior.

The headliner can be used to improve aesthetics inside the vehicle along with the indoor habitability. Further, it can prevent passenger head injuries in the event of a crash and increase passenger comfort. In addition, the application of low-thermal-conductivity vacuum insulation to the headliner reduces the heat loads and losses relative to conventional polyurethane (PU) materials, thus reducing the energy consumption required for heating and cooling the cabin. Figure 2 outlines the concept of reducing the heat load and the heat loss process in an EV. In general, vacuum insulating materials reduce the energy consumption of air-conditioners and heaters in EVs, increase the EV mileage, and reduce the thermal load on the headliner.

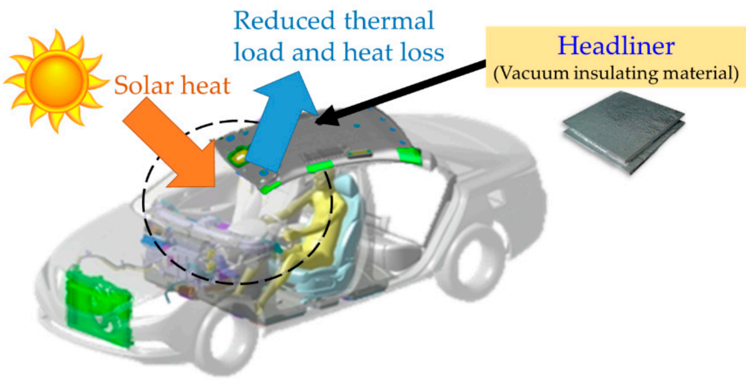

Figure 2. Concept to reduce heat load and heat loss in electric vehicles.

Figure 3 shows the product development process based on the insulation performance standard for automotive interior parts. First, the thermal conductivity and air permeability of the vacuum insulator material are evaluated. The prototype is next fabricated for parts evaluation. Finally, the headliner is mounted on the EV, and the actual vehicle is evaluated to experimentally verify the suitability.

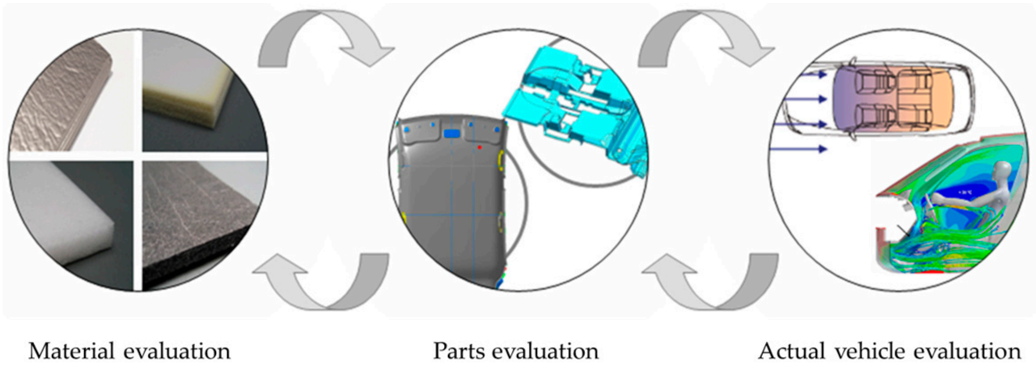

Figure 3. Product development process according to the evaluation method of insulation performance standard of automotive interior parts.

3. Experimental Verification

3.1. Material Evaluation

The materials currently used for automotive interior parts have diverse physical properties. To accurately confirm the thermal insulation performance for the fabrication of high-thermal-insulation components, we first identified the exact thermal characteristics of each normally used material. Four materials were selected for the evaluation: dry polyurethane (DPU); wet polyurethane (WPU); high-stiffness felt (HSFELT, and polypropylene glass fiber (PPGF). Figure 4 compares the thermal conductivities and air permeabilities of each material; in our study, DPU was chosen as the core of the conventional insulation model (hereafter the "conventional model") due to its lower air permeability relative to WET.

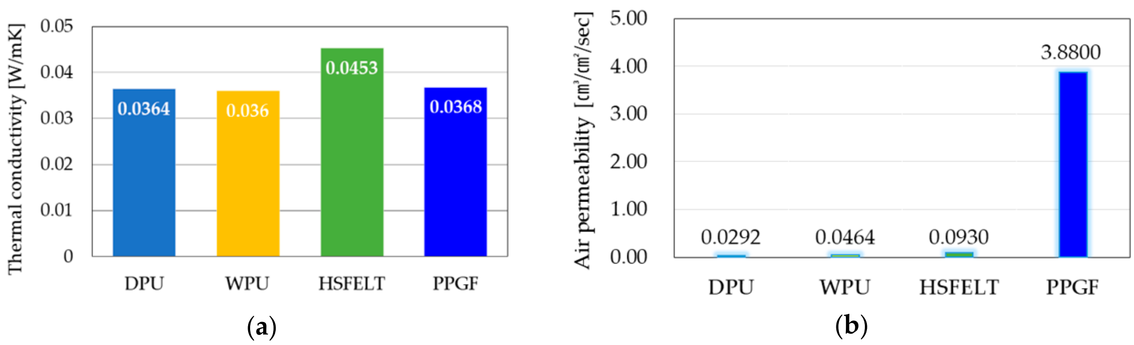

Figure 4. Comparison of thermal characteristics of each material considered: (**a**) Thermal conductivity; (**b**) Air permeability.

The thermal conductivity variation of DPU with temperature is shown in Figure 5. To improve the reliability of the results when measuring the insulation performance, we utilized the thermal conductivity values under the same temperature condition (25 °C) during evaluation.

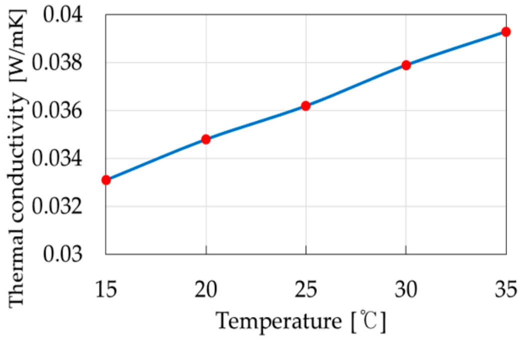

Figure 5. Thermal conductivity of dry polyurethane (DPU) material as function of temperature.

The vacuum insulation material used in the study was high-performance insulation with a thermal conductivity of <0.0045 W/mK, with vacuum evaporation realized within the insulation at less than 1 mbar. The resulting thermal insulation performance was −10 times better than that of conventional building vacuum insulation material whose thermal conductivity ranges from 0.031 to 0.045 W/mK. Since this vacuum insulation material has a low thermal conductivity, it is mainly used to improve the energy efficiency of buildings and devices such as refrigerators. Likewise, the vacuum insulation material can exhibit excellent insulation performance when applied to vehicles. In addition, because it is an inorganic insulating material, harmful and toxic gases are not generated in the event of a fire. Meanwhile, in the case of automotive interior parts, the appearance quality is very important; surface irregularities in the material can lead to mismatch with the peripheral parts, and thus the vacuum insulation material cannot function properly. Here, we note that the conventional model using the DPU core has the disadvantage of having an irregular surface because of the use of the common nylon film on the outer wall. To solve this problem, in the improved model using the vacuum insulation, we used a laminated heat-resistant polyolefin-based adhesive film on both sides of an aluminum-foil-laminated film with a thickness of 50 μm on a glass wool core material that was used as the vacuum insulation material. Figure 6 compares the surfaces of the conventional model with a DPU core and our improved model with the glass wool core.

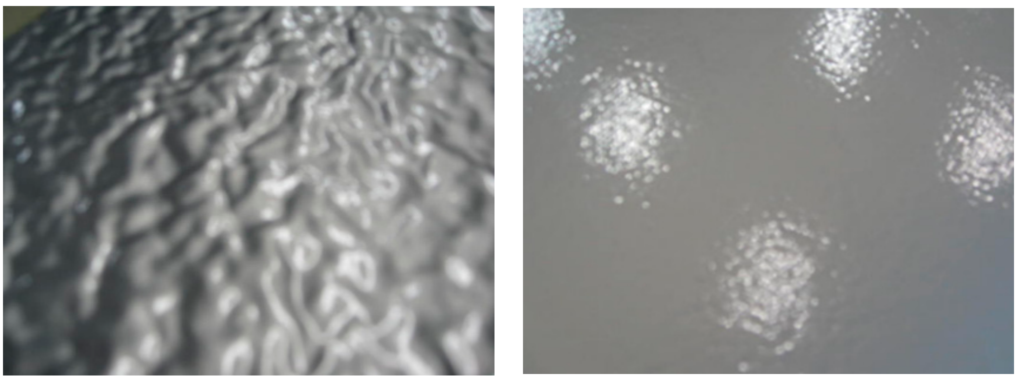

(**a**) (**b**)

Figure 6. Comparison of insulation surface: (**a**) Conventional; (**b**) Improved.

In the study, we tested the vacuum insulation materials based on IEA ECBCS Annex 39 [27,28]. The material thermal conductivity was measured according to the ISO 8302 standard [29]. The test used two identical specimens, and the thermal conductivity was measured by studying the temperature difference between the hot and cold surfaces, resulting from the application of a heater between the two specimens. The specimens were 200 mm × 200 mm in size and 10 mm thick. In the conventional model, the outer shell of the DPU core was composed of a nylon shell. In the proposed model (hereafter the "improved model"), the glass wool core was composed of the vacuum insulation of aluminum-foil-laminated film.

The thermal conductivities of the DPU and vacuum insulation materials were estimated to be 0.0364 W/mK and 0.0028 W/mK, respectively. Table 1 summarizes the quality improvement effect of the vacuum insulation material based on the surface quality improvement. The surface roughness listed in Table 1 is the value representing the difference between the heights of the highest and lowest points on the surface. A lower surface roughness corresponds to a smoother surface and better surface quality. Reducing the surface roughness reduced the likelihood of breaking the vacuum insulator when the skin layer was attached. In addition, the improved model used a glass wool core to lower the thermal conductivity and improve the thermal insulation performance.

Table 1. Comparison of characteristics of vacuum insulation material with surface quality improvement.

Items	Conventional	Improved	Unit
Surface roughness	100	5	μm
Thermal conductivity	0.0364	0.0028	W/mK

In general, a getter [30–33] is used within the vacuum insulator to absorb the generated moisture and maintain a high insulation performance for a long time. However, the getter is an inorganic material that has low elongation and elasticity. Therefore, when the vacuum insulation material is shaped, its skin layer can undergo damage along with the getter, which can drastically reduce the thermal insulation performance. Figure 7 shows that breakage that can occur during machining of the vacuum insulator for shaping.

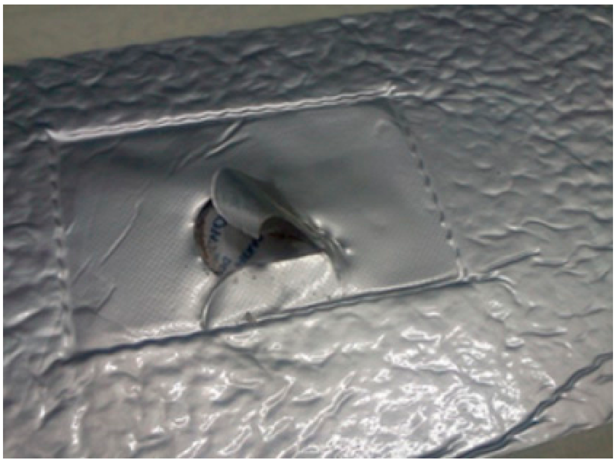

Figure 7. Breakage occurrence during shape machining of vacuum insulator.

We note that a glass wool core can only be used as the core for vacuum insulation materials after pretreatment. This is because glass wool has the form of a kind of fiber, and when used as-is, it can be easily deformed by an external force, and thus, its appearance cannot be maintained. Therefore, we applied compression pretreatment to glass wool. Since the outer wall is required to be in intimate contact with the core, the yarn or sheath used can protrude from the core surface during the introduction of the core and rub against the inner surface of the outer wall. For glass wool, due to the high hardness of the material itself, during this friction process, the inner surface of the outer wall can be damaged, which can lead to a high number of defects. Therefore, in order to prevent such defects, after the core is inserted into the outer wall, the outer wall is sealed under vacuum conditions to complete the manufacture of the vacuum insulation material. Consequently, the formability of the vacuum insulation material is improved, and the getter is uniformly formed as the core material. Figure 8 compares the formability improvement between the conventional and vacuum insulating materials.

The shaping possibilities for forming the vacuum insulation are increased, and any deflection due to the lack of load and rigidity of the headliner can be reduced.

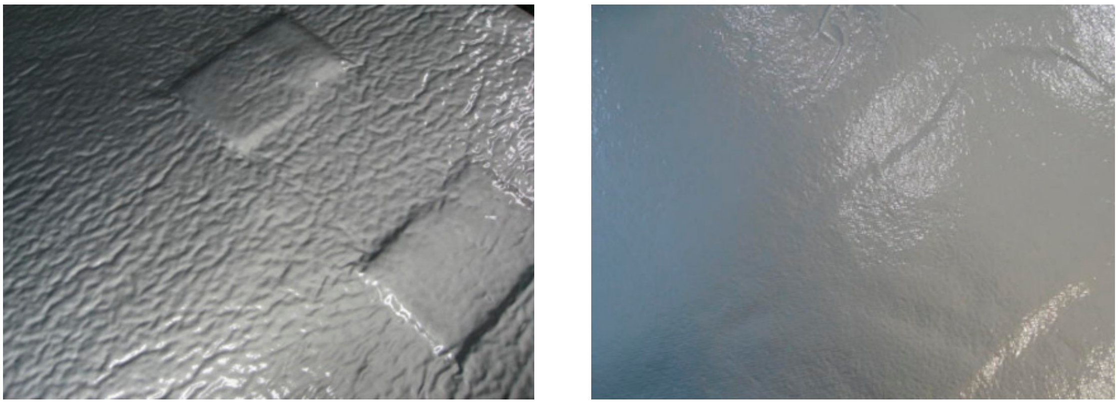

(**a**) (**b**)

Figure 8. Comparison of formability improvement: (**a**) Conventional; (**b**) Improved.

3.2. Parts Evaluation

Automotive headliners are composed of both skin and base layers. The skin layer of the headliner that uses a conventional PU composite board comprises a combination of knitted fabric and soft PU foam and hot melt film or nonwoven fabric and hot melt film. In our study, the improved model replaced the soft PU foam (area density: 104 g/m^2, density: 26 kg/m^3, thickness: 4 mm) of the skin layer with a melt-blown nonwoven fabric (area density: 80 g/m^2) that formed the vacuum insulation layer to reduce the thermal load. In addition, a polyethylene terephthalate (PET)-needle-punched nonwoven fabric (area density: 180 g/m^2) was applied to the substrate layer to increase the sound absorption area. Figure 9 shows the forming process of the headliner fabricated in this study as per the standard headliner manufacturing process. First, the substrate of the headliner is molded, and subsequently, the substrate is formed by cutting. The fabric attachment process is followed by attaching the knit fabric and nonwoven fabric to the substrate, and finally, the headliner is trimmed. Figure 10 shows the modeling and prototype of the headliner.

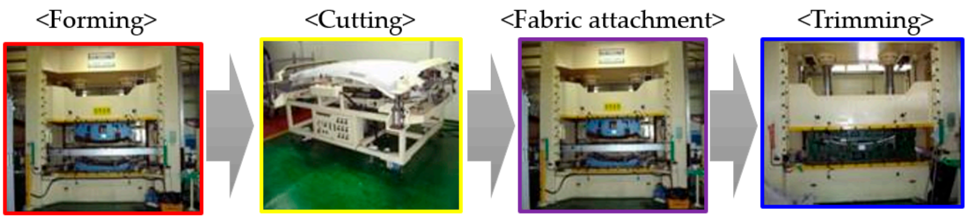

Figure 9. Forming process of headliner.

(**a**) (**b**)

Figure 10. Headliner: (**a**) Modeling; (**b**) Prototype.

Figure 11 shows the schematic of the headliner insulation performance evaluation facility, which consists of outdoor- and indoor-condition chambers. In the outdoor-condition chamber, I/O control was performed to replicate sunlight and the outdoor temperature conditions. The indoor-condition chamber was used to perform I/O control of the temperature of the indoor air and the heating and cooling airflow. The headliner parts for the evaluation were positioned between the outdoor-and indoor-condition chambers to measure and evaluate the heat transfer amount or thermal insulation performance.

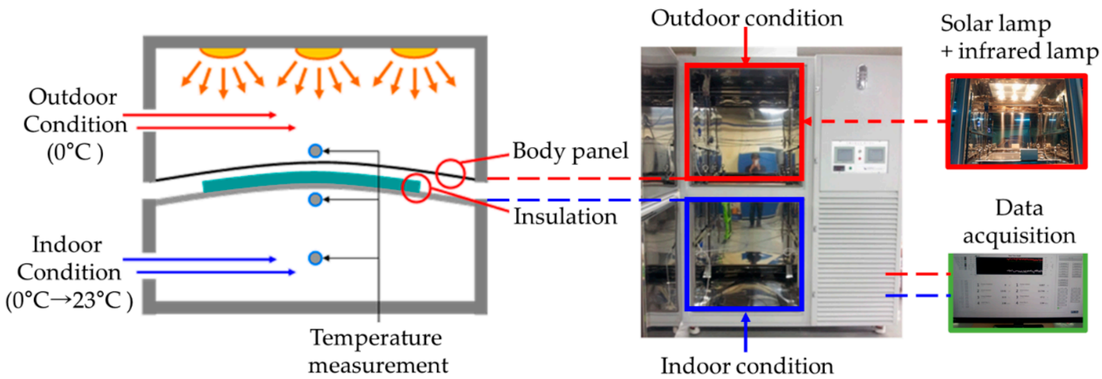

Figure 11. Configuration of headliner insulation performance evaluation facility.

Figure 12 shows the procedure for evaluating the headliner insulation performance. The purpose of the evaluation procedure was to identify the heating time required to change the indoor temperature condition from 0 °C to 23 °C and the time for which the indoor temperature was subsequently maintained. Therefore, the initial outdoor and indoor temperatures of the evaluation facility shown in Figure 11 were set to 0 °C; the outdoor temperature condition was maintained at 0 °C, and the indoor temperature condition was manually set to 23 °C, after which heating was applied. After the target temperature of 23 °C was reached, heating is stopped, and the time required to maintain this (room) temperature was recorded.

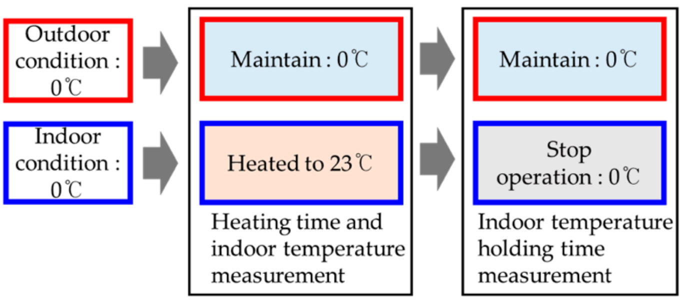

Figure 12. Evaluation procedure of headliner insulation performance.

Here, we note that for the evaluation the speed of the heated wind flowing into the indoor chamber upon heater operation had to be estimated. Figure 13a shows the increase in wind speed caused by the blower switching mechanism of an actual compact car, whereas Figure 13b shows the wind speed according to the blower output of the evaluation facility. In general, passengers use three to five "shifts" of the blower for heating. Thus, the blower of the evaluation facility should afford an output of 60 W to 100 W, and this output range was decided as the evaluation range in the study.

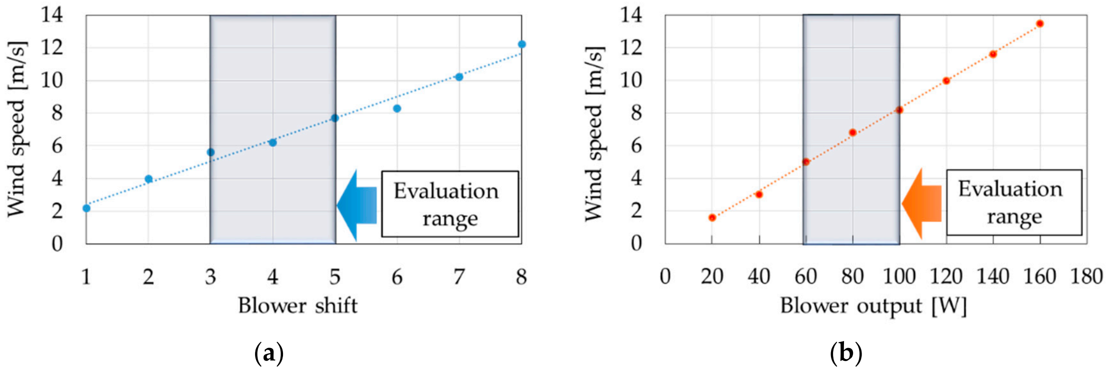

Figure 13. Comparison of wind speeds: (**a**) Blower of compact car; (**b**) Blower output of evaluation facility.

To reproduce the outdoor conditions under which the actual headliner is subjected to in terms of receiving solar energy, we mounted solar and infrared (IR) lamps to irradiate the headliner. Figure 14a shows the illumination intensities of the solar and IR lamps and the combined intensities according to the wavelength. We note that IR lamps are a type of incandescent lamp with enhanced IR radiation characteristics. Their input energy is emitted as infrared energy, with the visible light emitted being lower than that of solar lamps. Figure 14b shows the IR lamp irradiance as a function of the output. The output of the IR lamp for evaluation was determined to be 100%.

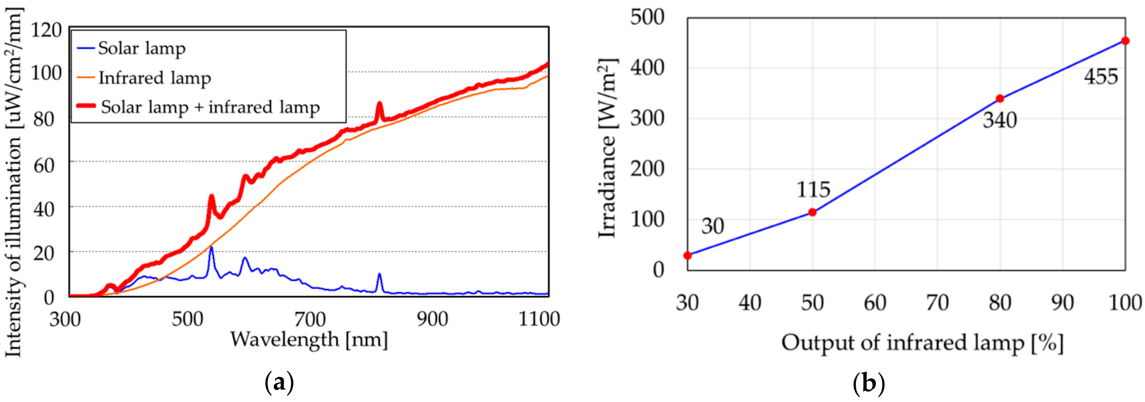

Figure 14. Intensity of illumination and irradiance: (**a**) Intensity of illumination according to wavelength; (**b**) Irradiance according to output of infrared lamp.

Table 2 lists the results of the headliner insulation performance evaluation. The evaluation was performed with a blower output of 100 W and IR lamp output of 100%. The heating temperature was set at 23 °C, and heating was applied until the indoor chamber temperature reached the set temperature. With the conventional model, 52 min of heating was required, whereas the improved model required only 45 min, corresponding to a time reduction of 15.5%. After heating was stopped, the indoor temperature holding time was measured as 150 s for the conventional model and 170 s for the improved model. The inner headliner temperature was 18.20 °C for the conventional model and 19.84 °C for the improved model. The temperature of the headliner was lower than the indoor temperature of 23 °C because the outdoor temperature was maintained at 0 °C. Thus, the insulation at the indoor temperature holding time of the improved model increased by 13.33% relative to the conventional model.

Table 2. Headliner insulation performance evaluation result.

Items	Conventional	Improved	Unit	Remark
Heating time up to indoor temperature 23 °C	52	45	Minute	Blower output: 100 W
Inner headliner temperature	18.20	19.84	°C	Infrared lamp output: 100%
Indoor temperature holding time	150	170	Second	-
Insulation effect at indoor temperature holding time	-	13.33	%	-

After the performance evaluation of the headliner, we conducted reliability tests to evaluate the feasibility of the improved model. Figure 15 shows the heat-resistant cycle profile applied for verifying the reliability of the headliner over 10 cycles of testing. Further, Figure 16 shows the images of the prototypes before and after the headliner reliability test. After completion of the heat cycle test, we confirmed that there was no structural abnormality. Table 3 lists the results of the reliability test. Surface density and flexural strength characteristics and the absence of deformation clearly meet the requirements in Table 3.

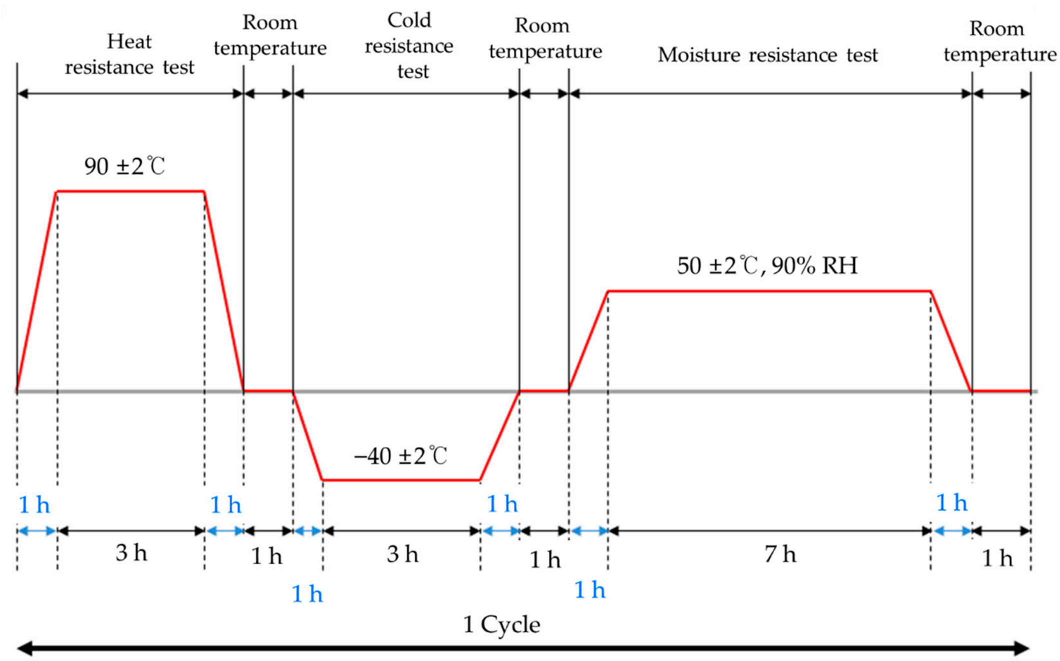

Figure 15. Heat-resistant cycle profile applied for verifying functional reliability of headliner.

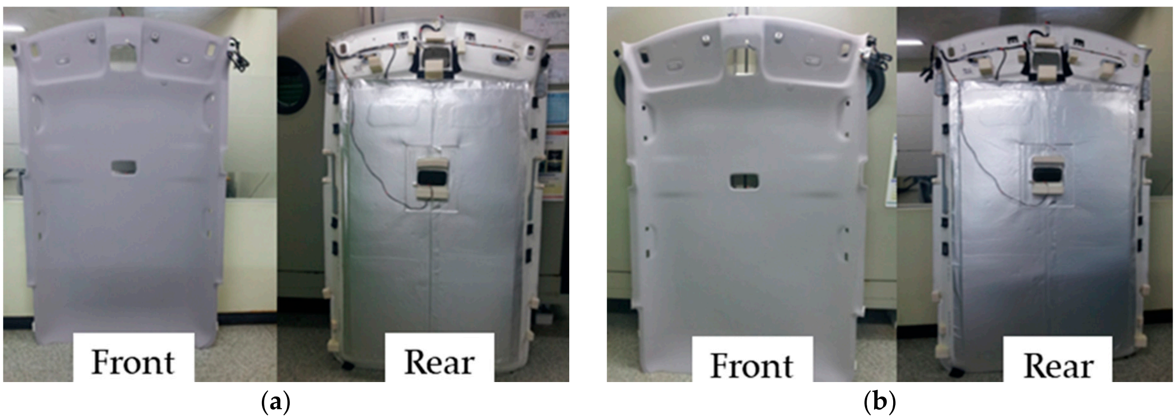

Figure 16. Prototype of the headlining reliability test: (**a**) Before; (**b**) After.

Table 3. Headlining insulation performance evaluation result.

Items	Requirements	Value	Unit
Surface density	Below 840	829.5	g/m^2
Flexural strength	Above 2.40	2.46	kgf/cm
Heat-resistant cycle	No deformation	Clear	-

3.3. Actual Vehicle Evaluation

Next, we evaluated the headliner insulation performance by mounting the headliner onto the actual vehicle. We assumed the following conditions for evaluating the actual vehicle heat load:

- IR is possible and testing is carried out in a chamber that can enter the vehicle.
- The IR irradiation conditions are based on the surface temperature of 100 °C on the vehicle roof panel.
- In summer, indoor temperature rise can occur due to sunlight.
- In order to check the indoor temperature increase due to sunlight in the summer, the outdoor temperature is maintained at 35 °C and the vehicle roof panel temperature is maintained at 100 °C.
- In summer, cooling starts after checking the room temperature rise due to outside parking.
- The winter season outdoor temperature is assumed as 0 °C in the absence of sunlight.
- The indoor air-conditioning is temperature 23 °C and the blower shift position is set to 5; the same blowing condition is applied for both cooling and heating.

Figure 17a shows the actual vehicle test environment, with Figure 17b showing the interior of a vehicle equipped with our thermal load evaluation equipment. The actual thermal load evaluation equipment affords the following features.

- Measurement and analysis of real-time indoor temperature.
- Remote up/down and left/right movement of the thermal imaging camera.
- Insulation cover that can be applied to prevent the thermal damage of the imaging camera.

(**a**) (**b**)

Figure 17. Actual vehicle evaluation environment: (**a**) Test environment; (**b**) Inside vehicle.

The actual thermal load evaluation results are shown in Figure 18. Figure 18a shows the indoor temperature characteristics in summer, whereas Figure 18b shows the indoor temperature characteristics in winter.

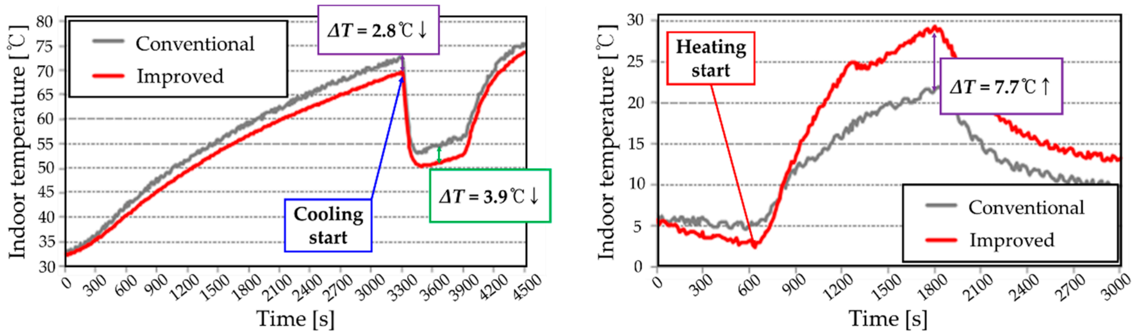

(**a**) (**b**)

Figure 18. Actual thermal load evaluation results: (**a**) Summer cooling evaluation result (indoor temperature); (**b**) Winter heating evaluation result (indoor temperature).

The results of the evaluation of actual heat load by season can be summarized as follows:

- In summer, the elevated indoor temperature is 2.8 °C lower under outdoor parking conditions.
- The indoor temperature is 3.9 °C lower than the conventional model for cooling outdoor vehicles in summer.
- The indoor temperature increases by 7.7 °C relative to the case of the conventional model when heating the vehicle outdoor in winter.

Figure 19 compares the surface temperatures (obtained using a thermal imaging camera) of the headliner between the conventional and improved models when the vehicle is left outdoors in the summer. Here, Sp1 indicates the headliner portion and Sp2 represents the part without the headliner; Table 4 lists the surface temperatures in the two cases. Overall, the improved model affords lower indoor temperatures than the conventional model. In particular, the thermal load characteristics showed an improvement reflected by a reduction of 7.6 °C in the Sp1 portion including the headliner.

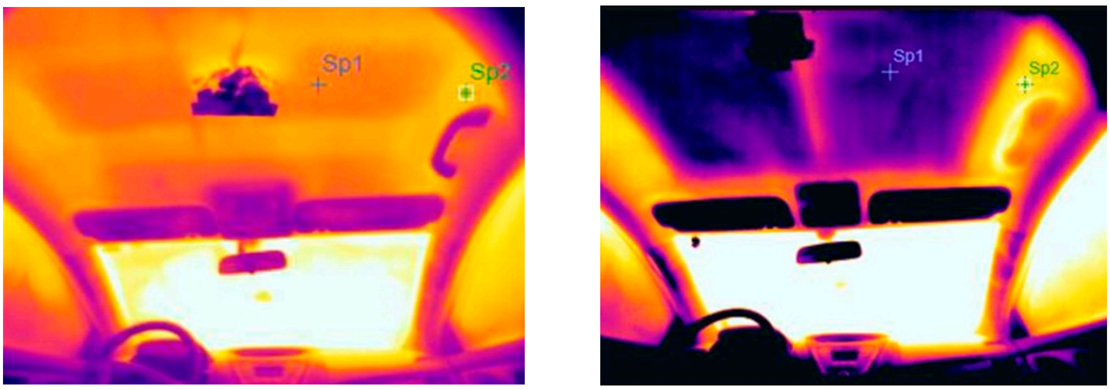

(**a**) (**b**)

Figure 19. Surface temperature of headliner upon leaving vehicle outdoors in summer (thermal camera measurements): (**a**) Conventional; (**b**) Improved.

Table 4. Comparison of surface temperature.

Items	Conventional	Improved	Unit	Remark
Headliner portion (Sp1)	65.5	57.9	°C	Reduced by 7.6 °C
Non-headliner portion (Sp2)	66.7	62.6	°C	Reduced by 4.1 °C

Next, we used an actual electric vehicle to confirm the improvement in battery power consumption and mileage resulting from vacuum insulation use. The actual driving evaluation was carried out using a compact-car-class EV equipped with our improved high-insulation vacuum headliner. Figure 20 shows the driving evaluation results of the vehicle together with the heating and cooling operation under the environmental conditions in winter and summer. We note that EVs have no energy-generating means besides batteries, and therefore, all onboard EV equipment use batteries. Therefore, to minimize the mileage reduction rate, efficient management of all functions using the battery in the EV is required. In the driving evaluation of the EV equipped with the improved high-insulation vacuum headliner, the battery power consumption was reduced by 6% for cooling and 7% for heating, as shown in Figure 20a. We hypothesize that the heat energy generated by the air-conditioner and heater was effectively blocked from "escaping" by the application of the high-insulation vacuum headliner. When the insulation within the vehicle was improved by the application of high-insulation vacuum headliner, the amount of electrical energy consumed for cooling or heating was reduced, and the distance that can be driven by one-time charging of the electric vehicle increased, as can be inferred from Figure 20b. When the high-insulation vacuum headliner was installed, the driving distance increased by 1.0% for cooling and 1.5% for heating relative to the conventional headliner.

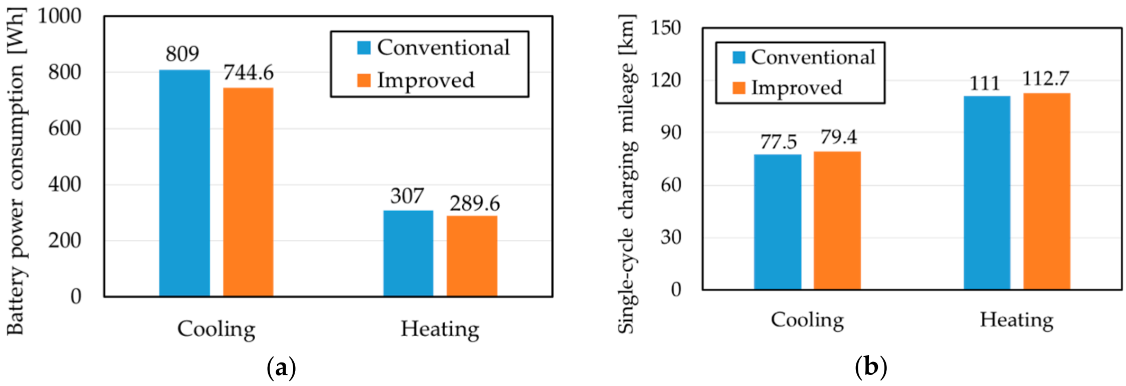

Figure 20. (**a**) Battery power consumption and (**b**) mileage resulting from one charge cycle with conventional and proposed headliners under cooling and heating conditions.

4. Conclusions

We experimentally verified the efficacy of using vacuum insulating material in the EV headliner to reduce thermal load. The insulating material, parts, and actual vehicle evaluations were performed according to the evaluation method of the insulation performance standard for automotive interior parts. We fabricated a headliner composed of vacuum insulation material with reduced surface roughness and thermal conductivity, which lead to improved thermal load handling. In addition, our improvements to the molding method ensured that the headliner structure was more resistant to breakage during processing. Experiments were conducted to evaluate the insulation performance of the headliner by considering the effects of solar heat and external wind; the resulting insulation performance exhibited a significant improvement over conventional insulation. Further, the material thermal conductivity was measured as per the ISO 8302 standard. Our reliability tests confirmed that the surface density, flexural strength, and heat resistance criteria were satisfied.

The EV thermal load was evaluated by installing the improved headliner in an actual vehicle, and we found that the indoor environment of the vehicle could be more comfortably maintained via effective management of the heat energy introduced from the outside environment and the heating and cooling energy generated indoors. As per the air-conditioning and heating evaluation, the indoor temperature was lowered by 2.8 °C during summer under outdoor parking conditions and 3.9 °C during cooling relative to the conventional headliner. In the case of heating during winter driving, the indoor temperature was 7.7 °C higher relative to the conventional headliner, which proved that the same amount of heating energy can be used to keep the cabin warm even in winter. Under the same conditions, the time required for air-conditioning and heating is reduced, and because the electrical energy used for air-conditioning is reduced, that available for driving increases. The mileage of the EV increased because of the improved insulation performance of the parts rather than the (light) weight of the parts.

Among the problems to be solved for the commercialization of EVs, the reduction in mileage caused by air-conditioning power consumption is a major concern. Currently, cars with vacuum insulation have not been mass-produced. We believe that the application of vacuum insulating material to headliners in mass-produced EVs can lead to significant energy savings.

Author Contributions: Conceptualization, S.-W.B.; Methodology, S.-W.B. and S.W.L.; Software, S.-W.B. and S.W.L.; Validation, S.-W.B. and S.W.L.; Writing—original draft preparation, S.-W.B.; Writing—review and editing, S.W.L.; and C.-S.K.; Supervision, C.-S.K.; Funding acquisition, S.-W.B.

Funding: This study was supported by the National Research Foundation of Korea (NRF) grant funded by the Korea government (MSIT) (No. 2017R1C1B5075525).

Conflicts of Interest: The authors declare no conflict of interest.

References

1. Loiselle-Lapointe, A.; Whittal, I.; Christenson, M. Electric Vehicles: Impacts of Mileage Accumulation and Fast Charging. *World Electr. Veh. J.* **2016**, *8*, 249–262. [CrossRef]
2. Botsford, C.W.; Edwards, A. An Integrated Global Philosophy of EV Charging. *World Electr. Veh. J.* **2016**, *8*, 495–500. [CrossRef]
3. Trentadue, G.; Lucas, A.; Otura, M.; Pliakostathis, K.; Zanni, M.; Scholz, H. Evaluation of Fast Charging Efficiency under Extreme Temperatures. *Energies* **2018**, *11*, 1937. [CrossRef]
4. Dost, P.K.; Spichartz, P.; Sourkounis, C. Charging Behavior of Users Utilizing Battery Electric Vehicles and Extended Range Electric Vehicles Within the Scope of a Field Test. *IEEE Trans. Ind. Appl.* **2018**, *54*, 580–590. [CrossRef]
5. Zhang, G.; Qin, F.; Zou, H.; Tian, C. Experimental Study on a Dual-parallel-evaporator Heat Pump System for Thermal Management of Electric Vehicles. *Energy Procedia* **2017**, *105*, 2390–2395. [CrossRef]
6. Zhang, G.; Zou, H.; Qin, F.; Xue, Q.; Tian, C. Investigation on an Improved Heat Pump AC System with the View of Return Air Utilization and Anti-fogging for Electric Vehicles. *Appl. Therm. Eng.* **2017**, *115*, 726–735. [CrossRef]
7. Kato, T.; Suzuki, R.; Miyao, R.; Kato, H.; Narita, T. A Fundamental Consideration of Active Noise Control System by Small Actuator for Ultra-Compact EV. *Actuators* **2018**, *7*, 49. [CrossRef]
8. Musat, R.; Helerea, E. Characteristics of the PTC Heater Used in Automotive HVAC Systems. *IFIP Adv. Inf. Commun. Technol.* **2010**, *314*, 461–468.
9. Shin, Y.H.; Ahn, S.K.; Kim, S.C. Performance Characteristics of PTC Elements for an Electric Vehicle Heating System. *Energies* **2016**, *9*, 813. [CrossRef]
10. Cho, S.; Jung, K.; Choi, J. Design Optimization of Interior Permanent Magnet Synchronous Motor for Electric Compressors of Air-Conditioning Systems Mounted on EVs and HEVs. *IEEE Trans. Magn.* **2018**, *54*, 1–5. [CrossRef]
11. Aziz, M.; Oda, T.; Ito, M. Battery-assisted charging system for simultaneous charging of electric vehicles. *Energy* **2016**, *100*, 82–90. [CrossRef]
12. Quddus, M.A.; Shahvari, O.; Marufuzzaman, M.; Usher, J.M.; Jaradat, R. A collaborative energy sharing optimization model among electric vehicle charging stations, commercial buildings, and power grid. *Appl. Energy* **2018**, *229*, 841–857. [CrossRef]
13. Collin, R.; Miao, Y.; Yokochi, A.; Enjeti, P.; von Jouanne, A. Advanced Electric Vehicle Fast-Charging Technologies. *Energies* **2019**, *12*, 1839. [CrossRef]
14. Jung, H.; Silva, R.; Han, M. Scaling Trends of Electric Vehicle Performance: Driving Range, Fuel Economy, Peak Power Output, and Temperature Effect. *World Electr. Veh. J.* **2018**, *9*, 46. [CrossRef]
15. Li, C.; Brewer, E.; Pham, L.; Jung, H. Reducing Mobile Air Conditioner (MAC) Power Consumption Using Active Cabin-Air-Recirculation in A Plug-In Hybrid Electric Vehicle (PHEV). *World Electr. Veh. J.* **2018**, *9*, 51. [CrossRef]

16. Wei, C.; Hofman, T.; Ilhan Caarls, E.; van Iperen, R. Integrated Energy and Thermal Management for Electrified Powertrains. *Energies* **2019**, *12*, 2058. [CrossRef]
17. Kwon, C.; Lee, C.W.; Foster, L.; Kwon, J.; Shin, Y. Development of an energy-saving occupied-zone HVAC system (OZ HVAC). In Proceedings of the SAE 2012 World Congress & Exhibition, Detroit, MI, USA, 24–26 April 2012.
18. Tabei, K.; Watanabe, M.; Doi, N.; Imai, K.; Young, S. Development of a S-FLOW System and Control (S-FLOW: Energy Saving Air Flow Control System. In Proceedings of the SAE 2013 World Congress & Exhibition, Detroit, MI, USA, 16–18 April 2013.
19. Wang, M.; Wolfe, E.; Ghosh, D.; Bozeman, J.; Chen, K.H.; Han, T.; Zhang, H.; Arens, E. Localized cooling for human comfort. *SAE Int. J. Passeng. Cars Mech. Syst.* **2014**, *7*, 755–768. [CrossRef]
20. Dolgopolsky, I.; Duley, J.A. Polyurethane Foam as an Integral "Core" Component of Automotive Headliner. *J. Ind. Text.* **2000**, *30*, 26–41.
21. Parikh, D.V.; Chen, Y.; Sun, L. Reducing Automotive Interior Noise with Natural Fiber Nonwoven Floor Covering Systems. *Text. Res. J.* **2006**, *76*, 813–820. [CrossRef]
22. Da Silva, C.; Calçada, M.; Massarelli, L. *Vehicle Interior Noise Reduction Using Innovative Roof Trim Structure*; SAE Technical Paper 2014-36-0767; SAE International: Warrendale, PA, USA, 2014. [CrossRef]
23. Kwon, J.-S.; Jang, C.H.; Jung, H.; Song, T.-H. Effective thermal conductivity of various filling materials for vacuum insulation panels. *Int. J. Heat Mass Transf.* **2009**, *52*, 5525–5532. [CrossRef]
24. Peng, C.; Yang, J. Structure, Mechanism, and Application of Vacuum Insulation Panels in Chinese Buildings. *Adv. Mater. Sci. Eng.* **2016**, *2016*. [CrossRef]
25. Kim, J.H.; Kim, S.M.; Kim, J.T. Simulation performance of building wall with vacuum insulation panel. *Procedia Eng.* **2016**, *180*, 1247–1255. [CrossRef]
26. Biswas, K.; Desjarlais, A.; Smith, D.; Letts, J.; Yao, J.; Jiang, T. Development and thermal performance verification of composite insulation boards containing foam-encapsulated vacuum insulation panels. *Appl. Energy* **2018**, *228*, 1159–1172. [CrossRef]
27. Simmler, H.; Brunner, S.; Heinemann, U.; Schwab, H.; Kumaran, K.; Mukhopadhyaya, P.; Quenard, D.; Sallee, H.; Noller, K.; Kucukpinar-Niarchos, E.; et al. Vacuum Insulation Panels: Study on VIP-components and Panels for Service Life Prediction of VIP in Building Applications (Subtask A). *IEA/EBC Annex 39* **2005**, *39*, 1–159.
28. Binz, A.; Moosmann, A.; Steinke, G.; Schonhardt, U.; Fregnan, F.; Simmler, H.; Brunner, S.; Ghazi Wakili, K.; Bundi, R.; Heinemann, U. Vacuum Insulation in the Building Sector-Systems and Applications (Subtask B). *IEA/EBC Annex 39* **2005**, *39*, 1–134.
29. ISO 8302 Standard: 1991(R2013). *Thermal Insulation—Determination of Steady-State Thermal Resistance and Related Prosperities—Guarded Hot Plate Apparatus*; International Organization for Standardization: Geneva, Switzerland, 1991.
30. Manini, P. Recent Developments in the Open Cell Foam-Filled Vacuum Insulated Panels for Appliances Applications. *J. Cell. Plast.* **1999**, *35*, 403–420. [CrossRef]
31. Brunner, S.; Simmler, H. In Situ Performance of Vacuum Insulation Panels in a Flat Roof Construction. *Vacuum* **2007**, *82*, 700–707. [CrossRef]
32. Chuntonov, K.; Ivanov, A.O.; Verbitsky, B.; Setina, J. Getters for vacuum insulated glazing. *Vacuum* **2018**, *155*, 300–306. [CrossRef]
33. Memon, S.; Farukh, F.; Kandan, K. Effect of Cavity Vacuum Pressure Diminution on Thermal Performance of Triple Vacuum Glazing. *Appl. Sci.* **2018**, *8*, 1705. [CrossRef]